



EXTINCTION

The marine biodiversity impact of the Late Miocene Mediterranean salinity crisis

Konstantina Agiadi^{1*}, Niklas Hohmann^{2,3}, Elsa Gliozzi⁴, Danae Thiviou^{5,6}, Francesca R. Bosellini⁷, Marco Taviani^{8,9}, Giovanni Bianucci¹⁰, Alberto Collareta¹⁰, Laurent Londeix¹¹, Costanza Faranda⁴, Francesca Bulian^{12,13}, Eferpi Koskeridou⁶, Francesca Lozar¹⁴, Alan Maria Mancini^{14,15}, Stefano Dominici¹⁶, Pierre Moissette⁶, Ildefonso Bajo Campos¹⁷, Enrico Borghi¹⁸, George Iliopoulos¹⁹, Assimina Antonarakou⁶, George Kontakiotis⁶, Evangelia Besiou⁶, Stergios D. Zarkogiannis²⁰, Mathias Harzhauser²¹, Francisco Javier Sierra¹², Marta Coll²², Iuliana Vasiliev²³, Angelo Camerlenghi²⁴, Daniel García-Castellanos²⁵

Massive salt accumulations, or salt giants, have formed in highly restricted marine basins throughout geological history, but their impact on biodiversity has been only patchily studied. The salt giant in the Mediterranean Sea formed as a result of the restriction of its gateway to the Atlantic during the Messinian Salinity Crisis (MSC) 5.97 to 5.33 million years ago. Here, we quantify the biodiversity changes associated with the MSC based on a compilation of the Mediterranean fossil record. We conclude that 86 endemic species of the 2006 pre-MSC marine species survived the crisis, and that the present eastward-decreasing richness gradient in the Mediterranean was established after the MSC.

The Messinian Salinity Crisis (MSC) represents a relatively recent severe environmental and landscape change (1, 2) involving the isolation and alternating hyper- and hyposalinization of the Mediterranean Sea (3) (Fig. 1) between 5.97 and 5.33 million years ago (Ma). The Mediterranean Sea is a large marginal sea at mid-latitudes that functions as a biodiversity hotspot refuge for hundreds of marine species. It ac-

quired its present semienclosed form in the Middle Miocene (~13.8 Ma) with the closure of the marine gateway connecting it to the Indian Ocean (4). In the Late Miocene, tectonic uplift of the former marine gateway areas to the Atlantic, in present-day southern Spain and northern Morocco, led to the disconnection of the basin (5–7). The restriction initiated in the latest Tortonian ~7.6 Ma (7) and accentuated during the Early Messinian from 7.17 Ma (8), causing strong salinity and temperature fluctuations in the Mediterranean and stratification of the water column (9, 10). Salt started depositing at 5.97 Ma, and complete disconnection was achieved at 5.6 Ma (11). The crisis ended with the opening of the Gibraltar straits and flooding of the Mediterranean basin with Atlantic water at 5.33 Ma (12). The MSC caused the accumulation of ~1 million km³ of salt in the Mediterranean (1), a kilometer-scale sea-level drop as a result of net evaporation exceeding precipitation and runoff (13), and a 5 parts per thousand decrease in the salinity of the global ocean (14). Despite the magnitude of these events, their biological impact at the ecosystem level remains relatively unknown.

Previous studies on the repercussions of the MSC and its precursor events (15) focused on specific groups of organisms, but these studies were based on incomplete and still uncertain scenarios about the course of events of the MSC. For some groups, such as tropical, reef-building corals, the MSC resulted in their complete extirpation from the Mediterranean (16). Moreover, whether these events shaped the present-day northwest-to-southeast decreasing trend in species richness in the Mediterranean (17) is still unknown.

We aimed to determine whether the MSC could have eradicated the Mediterranean ma-

rine biota by quantifying changes in species richness and beta diversity (species turnover and nestedness) before and after the MSC. Beta diversity represents the dissimilarity between two biota (total dissimilarity estimated here using the Sørensen index), which results from two processes, the replacement of species by different ones (species turnover estimated here using the Simpson index) and species loss through extinction (nestedness) (18, 19). We used 80% rarefaction to account for differences in sampling effort between the regions and intervals. Based on a recently compiled, updated fossil record of calcareous nannoplankton, dinoflagellates, planktic and benthic foraminifera, ostracods, corals, bivalves, gastropods, other mollusks, bryozoans, echinoids, fishes, and marine mammals (20, 21), we tested the hypotheses that: (i) species richness dropped during the Messinian, even before the MSC, in response to the ongoing marine gateway restriction as a result of the long-term inability of marine organisms to cope with the resulting paleoceanographic changes; (ii) the Tortonian (11.63 to 7.25 Ma), pre-evaporitic Messinian (7.25 to 5.97 Ma), and Zanclean (5.33 to 3.6 Ma) marine biota were dissimilar in taxonomic composition; and (iii) a northwest-to-southeast gradient in species richness was established after the MSC. The compiled record includes 22,932 verified occurrences of 4897 identified marine species in three Mediterranean regions, the Western Mediterranean, Eastern Mediterranean, and the Po Plain–Northern Adriatic (Fig. 1) from the Tortonian, the pre-evaporitic Messinian, and the Zanclean stages. Although there are ongoing controversies regarding the exact mechanisms at play during the MSC (22, 23) and the nature of the Mediterranean water bodies during the final stage of the crisis (24–26), our approach assesses the overall impact of the Messinian isolation of the Mediterranean and the MSC on marine biota.

A Zanclean restructuring of Mediterranean biodiversity

The results of the meta-analysis of the revised fossil record show that diversity was decreasing before the onset of evaporite precipitation and then recovered partially (one-tailed Mann-Whitney *U* test comparing subsampled species richness in Tortonian versus pre-evaporitic Messinian and pre-evaporitic Messinian versus Zanclean; in both cases, $P < 2.2 \times 10^{-16}$) after its termination with the arrival of species from the Atlantic and the Paratethys (24, 27, 28). Species richness overall dropped by 14.4% from the Tortonian to the Messinian (first and third quartile: 15.2 and 13.6%, respectively), but it increased again by 6.4% in the Zanclean (first and third quartile: 4.8 and 6.4%, respectively). A net decrease in species richness of 8% occurred from the Tortonian to the Zanclean (Fig. 2B).

¹Department of Geology, University of Vienna, Josef-Holaubek-Platz 2, 1090 Vienna, Austria. ²Faculty of Geosciences, Department of Earth Sciences, Utrecht University, 3584 CB Utrecht, Netherlands. ³Institute of Evolutionary Biology, University of Warsaw, 00-927 Warsaw, Poland. ⁴Dipartimento di Scienze, Università Roma Tre, 1-00146 Roma, Italy. ⁵Natural History Museum of Basel, 4001 Basel, Switzerland. ⁶Department of Historical Geology – Palaeontology, National and Kapodistrian University of Athens, Panepistimiopolis, 15784 Zografou, Greece. ⁷Dipartimento di Scienze Chimiche e Geologiche, Università degli Studi di Modena e Reggio Emilia, 09124 Cagliari, Italy. ⁸Institute of Marine Sciences – National Research Council (ISMAR-CNR), 40129 Bologna, Italy. ⁹Stazione Zoologica 'Anton Dohrn', 80122 Napoli, Italy. ¹⁰Dipartimento di Scienze della Terra, Università di Pisa, 56126 Pisa, Italy. ¹¹UMR 'EPOC' CNRS 5805, Université de Bordeaux, 33615 Pessac Cedex, France. ¹²Department of Geology, University of Salamanca, 37008 Salamanca, Spain. ¹³Groningen Institute of Archaeology, University of Groningen, 9712 Groningen, Netherlands. ¹⁴Department of Earth Sciences, University of Torino, 10125 Torino, Italy. ¹⁵Department of Life and Environmental Science, Università Politecnica delle Marche, 60122 Ancona, Italy. ¹⁶Museo di Storia Naturale, Università degli Studi di Firenze, 50121 Florence, Italy. ¹⁷Sección de Paleontología, Museo de Alcalá de Guadaíra, 41500 Seville, Spain. ¹⁸Società Reggiana di Scienze Naturali, 42122 Reggio Emilia, Italy. ¹⁹Department of Geology, University of Patras, University Campus, 26504 Achaia, Greece. ²⁰Department of Earth Sciences, University of Oxford, OX1 3AN Oxford, UK. ²¹Natural History Museum Wien, 1010 Vienna, Austria. ²²Institut de Ciències del Mar (ICM-CSIC), 08003 Barcelona, Spain. ²³Senckenberg Biodiversity and Climate Research Centre (BiK-F), 60325 Frankfurt am Main, Germany. ²⁴OGS Istituto Nazionale di Oceanografia e di Geofisica Sperimentale, 34010 Trieste, Italy. ²⁵Geosciences Barcelona (GEO3BCN-CSIC), 08028 Barcelona, Spain. *Corresponding author. Email: konstantina.agiadi@univie.ac.at

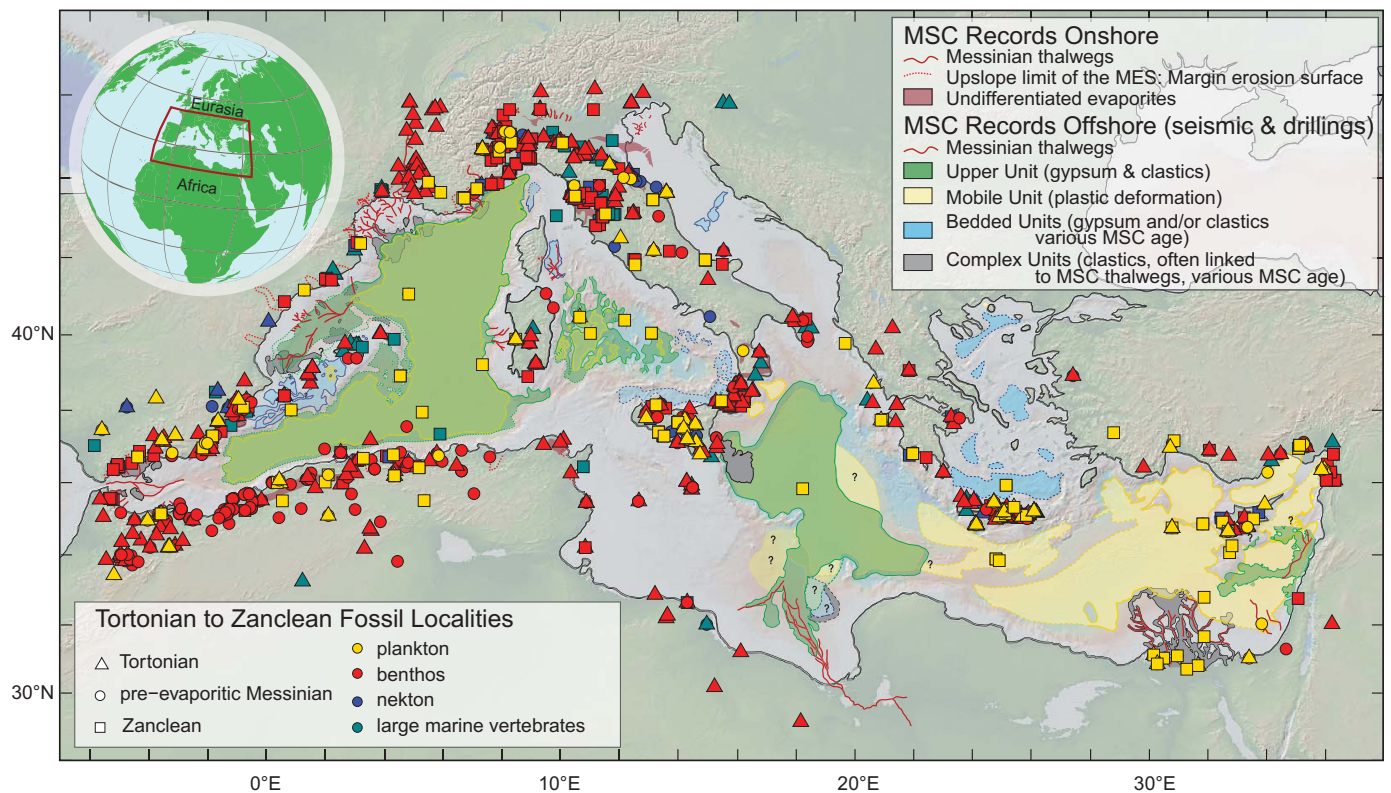


Fig. 1. Map of the Mediterranean area with the fossil localities included in the analysis. Plankton includes calcareous nannoplankton, dinoflagellates, and planktic foraminifera. Benthos includes benthic foraminifera, ostracods, corals, bivalves, gastropods, other mollusks, bryozoans, and echinoids. Nekton includes bony fishes.

Large marine vertebrates include sharks and marine mammals. Background information on the MSC (units distinguished in seismic profiles, onshore observed evaporites, and Messinian thalwegs or water courses) were obtained from (69). The dataset, including references and locality information, is available in (20).

The Zanclean recovery at the basin scale was driven by the Western Mediterranean, whereas Po Plain–Northern Adriatic and, more so, Eastern Mediterranean species richness continued to decline (fig. S1).

Simultaneously, the taxonomic composition of the Mediterranean marine biota changed: Tortonian and pre-evaporitic Messinian biota were 50.4% dissimilar (first and third quartile: 50 and 50.7%, respectively), whereas Tortonian and Zanclean biota were 66.8% dissimilar (first and third quartile: 66.5 and 67.3%, respectively; Fig. 2D). Species turnover accounts for most of these changes, whereas nestedness remains in all comparisons below 5%, indicating that most of the change resulted from the introduction of new species in the basin after the MSC rather than the reestablishment or survival of pre-MSC species and ecosystems.

Of the 2006 distinct marine species, both endemic and nonendemic, recorded from the pre-evaporitic Messinian, at maximum, only 86 endemic species apparently survived into the Pliocene, whereas 693 possible endemic Mediterranean species disappeared (29). Because of the incompleteness of the fossil record, it is impossible to know if an extinct species has been endemic. Therefore, these values are conservative estimates based on the Mediterranean

fossil record analyzed here (20, 21) and the current state of knowledge about the species' paleobiogeographic distributions (29). Several of the species considered to be endemic are suspected to be misidentifications, but their records in the literature were presented without photographs and the corresponding specimens are not available in collections (20, 21), so their identity cannot be verified. The rest of the species are believed to have found refuge during the peak of the crisis in the Atlantic adjacent to the Mediterranean, although fossil records are scarce (30, 31). Few marine species have been reported from the first stage of the MSC (5.97 to 5.6 Ma) (32). Even fewer marine species have been recorded from the last stage (5.5 to 5.33 Ma), where they are accompanied by fresh- and brackish-water species immigrating from the Paratethys (24, 26, 32). Overall, the analysis of the fossil record before and after the MSC points to extirpation of the Mediterranean biota during the crisis.

The MSC impact on Mediterranean biodiversity is not comparable to past global mass extinction events or even to present-day anthropogenic impacts. Mediterranean biodiversity today is disproportionately high relative to the size of the basin because of its

numerous endemic species (17). Our results suggest that this was true also in the Late Miocene, but most of those endemics disappeared in the Messinian. In this respect, the MSC reduced global biodiversity, although an equivalent worldwide fossil record for that period is not available to quantify the magnitude of this impact. We can compare the impact of the MSC to other similar regional transformations of marine biota, such as the Central Paratethys evaporitic basin (approximately the Black Sea basin) in the latest Middle Miocene (~12.65 Ma) that resulted from the influx of brackish water from the Eastern Paratethys, the subsequent connection with the Mediterranean, and the establishment of marine conditions (33). The magnitude of change during these events appears to be similar to the MSC-related changes. For example, the potamidid gastropod faunas in both cases are >60% dissimilar between the time intervals before and after the gateway reconstructions (34, 35).

Spatial redistribution of Mediterranean marine species

Today, the Mediterranean Sea biota exhibit a southeastward decreasing gradient in species richness that has been variously thought to be

associated with changing temperature, salinity, productivity, or distance from the Atlantic connection at Gibraltar (17), yet the origins of this modern gradient remain obscure. The post-MSC biodiversity patterns observed here indicate that such a gradient was first estab-

lished after the Zanclean flood (12) ~5.33 million years ago (Fig. 2). In the Tortonian, the larger Eastern Mediterranean contained 6% more species than the Western Mediterranean, a percentage that increased in the Messinian. By contrast, after the MSC, in the Zanclean,

Eastern Mediterranean contained 14% fewer species than the Western Mediterranean. In addition, the Po Plain–Northern Adriatic region showed greater species richness than both the Eastern and Western Mediterranean in the Tortonian [when it was still connected to the latter (36)] and the Messinian (fig. S1), even though it is the smallest of the three regions (37). Species richness in the Po Plain–Northern Adriatic remains almost constant across the transition to the Pliocene. These results support the establishment of a northwest-to-southeast decreasing gradient in species richness across the Mediterranean Sea during the Zanclean, which is in contrast to the hypotheses that the gradient today results solely from its distance from Gibraltar or from a sea surface temperature gradient. The connection to the Indian Ocean was severed ~13.8 Ma, leaving the Atlantic as the only source of new diversity for several millions of years before the MSC (4). The Eastern Mediterranean was located south of the Western sub-basin throughout the Miocene (38), so the sea surface temperature would be expected to be higher in the Eastern than in the Western Mediterranean. However, by the Tortonian, the biodiversity gradient did not exist (Fig. 2). It is possible that seawater salinity, productivity, the oceanic circulation with the Atlantic and within the basin, or a combination of these factors contributed to the biodiversity gradient, but pre-Tortonian data are not currently available to test such hypotheses. Until the Tortonian, the Western Mediterranean was much smaller than the Eastern Mediterranean, whereas the difference became less pronounced in the Messinian and Zanclean. Additionally, the intermittent connection of the Eastern Mediterranean with the Paratethys basins throughout the Miocene (38) drove the origination of a rich endemic fauna in the former [e.g., (39)], thereby increasing species richness before the MSC. The currently available fossil record does not offer evidence for the gradient remaining continuously from the Early Pliocene until today, but our results indicate that this pattern was sustained for at least 1.7 million years after the MSC until the end of the Zanclean (40).

Impact of the salt giant formation on marine biota

The changing configuration of gateways between marine basins determines not only the occurrence of abrupt salinity changes and the regional sea levels, but also the migration pathways of marine organisms and the flow of larvae and genes, thus controlling the structure and functioning of ecosystems and ultimately driving their evolution. In essence, gateway restriction and reopening, and evaporite formation itself, presumably caused large-scale disruption of functional processes, including population connectivity, plankton and larval

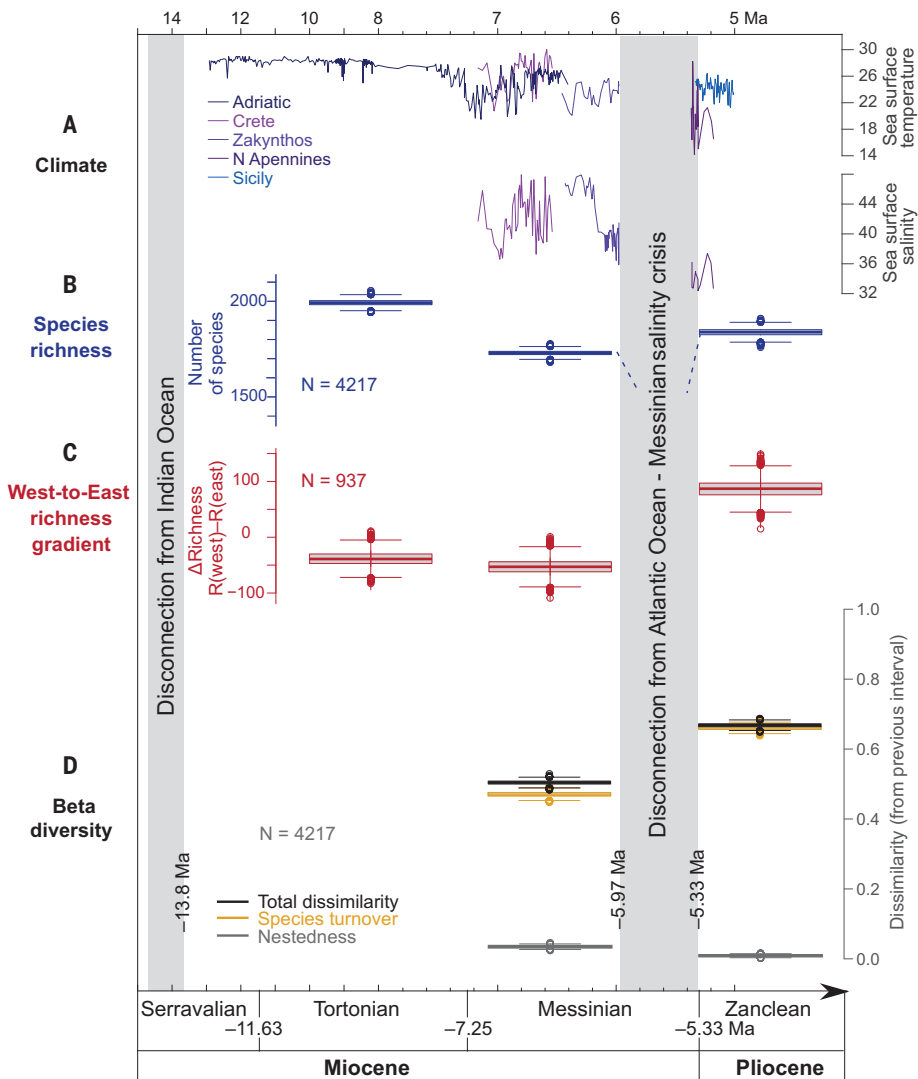


Fig. 2. Tortonian–Zanclean biodiversity changes in the Mediterranean Sea. (A and B) The restriction of the Mediterranean–Atlantic gateways caused high-amplitude temperature and salinity variations (A), which resulted in a decrease of species richness (B) in the pre-evaporitic Messinian (one-tailed Mann-Whitney *U* test comparing subsampled species richness in Tortonian versus pre-evaporitic Messinian; $P < 2.2 \times 10^{-16}$). Only partial recovery was achieved after the Messinian salinity crisis. (C) Species richness was lower in the Western than in the Eastern Mediterranean before (negative Δ Richness for both Tortonian and pre-evaporitic Messinian; one-sample, one-tailed Wilcoxon test; $P < 2.2 \times 10^{-16}$) but higher after the MSC (positive Δ Richness for Zanclean; $P < 2.2 \times 10^{-16}$). (D) Dissimilarity was high between the Tortonian and Messinian biota, as well as between the Messinian and Zanclean biota, and it was almost exclusively attributed to species replacement (turnover) rather than species loss (nestedness). *N* indicates the number of occurrences after subsampling to 80% of the smallest sample 10,000 times. In the boxplots, the bold line indicates the median value, the box corresponds to the quartiles (values included fall within 25th and 75th percentiles of the data), and the whiskers are quartiles ± 1.5 times the interquartile range. The data for sea surface temperature were based on the $U^{K_{37}}$ [Adriatic Sea (70); Sicily (71); Zakynthos, Ionian Sea (42); North Apennines (51)] and TEX_{86} indices [Crete, Eastern Mediterranean (10)]. Sea surface salinity was obtained by coupling the $\delta^{18}O$ of planktic foraminifera with $U^{K_{37}}$ [Zakynthos (42); North Apennines (51)] or TEX_{86} -based sea surface temperature [Crete, Eastern Mediterranean (10)]. For visualization, different scales for the time axis were used before and after 8 Ma.

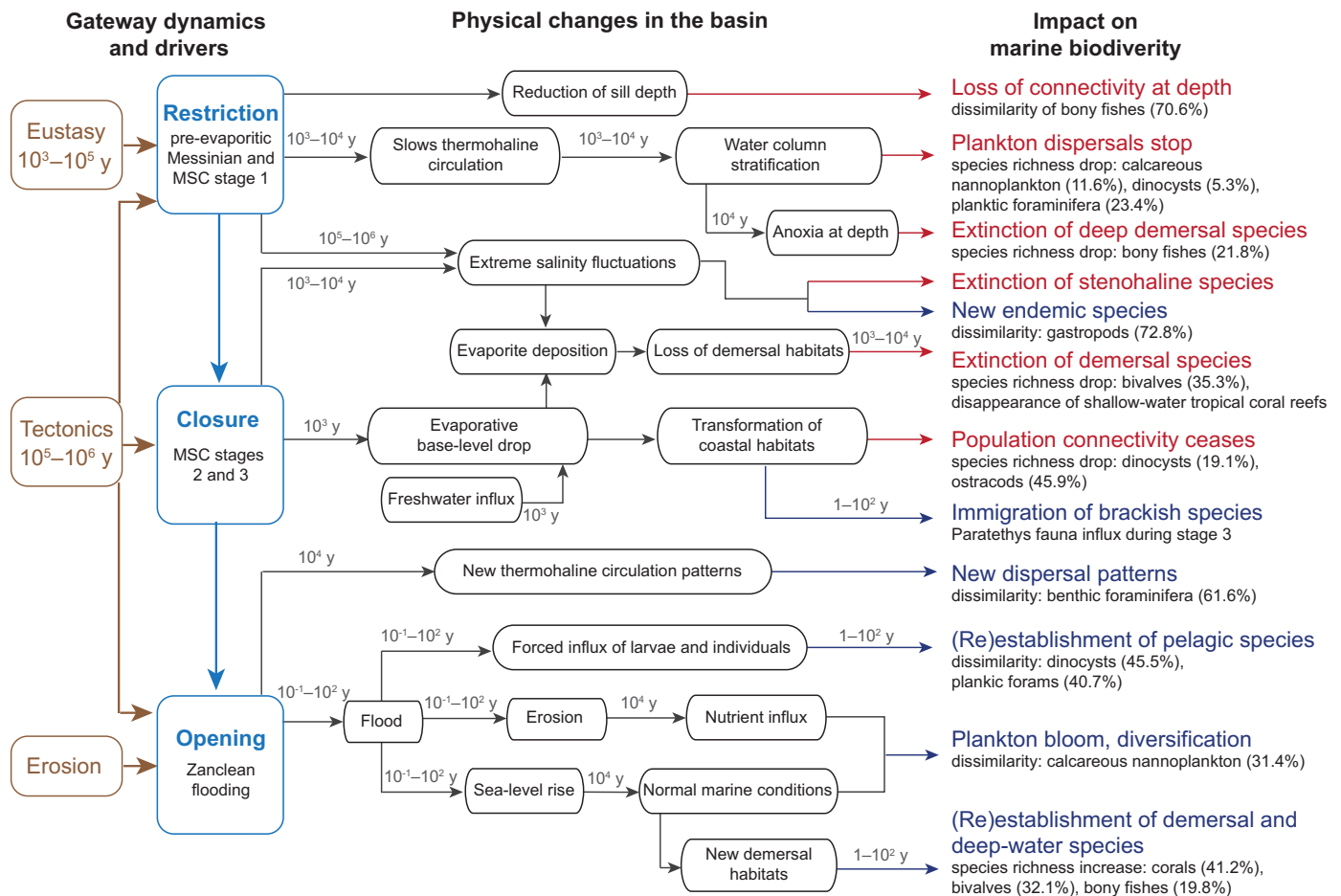


Fig. 3. Conceptual model of biodiversity impact of salt giant formation in the Mediterranean during the MSC. Gateway dynamics controlled the connectivity of the basin with the global ocean and affected marine biota. The range assigned to each arrow refers to the timescale in years at which each process took place wherever estimates are available. The examples for different

groups of organisms are derived from (34). Dissimilarity here refers to total dissimilarity resulting from both species replacement and species loss resulting from each physical change. Blue arrows indicate impacts that contributed to increases in biodiversity, and red arrows point to those that contributed to declines.

dispersal, vertical migration, seasonal migrations (latitudinal and longitudinal), land-to-sea connectivity, and coastal-to-deep connectivity (41). Based on our analysis of the revised fossil record, we have devised a conceptual model of the impact of the MSC on Mediterranean marine biodiversity (Fig. 3).

Our results are limited by the quality and size of the fossil record available. Gaps in the record vary by group and can be attributed to the spatiotemporal distribution of the sedimentary facies and the socioeconomic and political conditions in the peri-Mediterranean areas (21). In general, the distribution of the localities is skewed toward the north and west (Fig. 1). The Mediterranean Neogene marine deposits are among the best studied in terms of taxonomic paleontological and stratigraphic work, and the revision of the Tortonian–Zanclean record (20) resulted in a very high-quality record. Nevertheless, the resolution of the record does not allow for estimation of certain timescales in the model (Fig. 3), spe-

cifically the amounts of time between: (i) physical disconnection between Atlantic and Mediterranean populations and the extinction of species or the evolution of new endemic species; (ii) anoxia at depth and the extinction of deep demersal species; (iii) drawdown in the Mediterranean and the immigration and establishment of brackish-water species in the former marine areas; and (iv) the reactivation of thermohaline circulation in the basin and the establishment of new dispersal patterns of benthic and planktic organisms after the Miocene/Pliocene boundary transition.

Gateway restriction

A direct result of the restriction of the connection to the Atlantic was the loss of functional connectivity with the Mediterranean basin at depth. This was confirmed by the replacement of common cosmopolitan meso- and bathypelagic fish species by Mediterranean endemics, which contributed to the dissimilarity (70.6%) seen among the Tortonian and

pre-evaporitic Messinian fish faunas, the highest among the groups that we have examined (34). Salinity excursions [periods of hyper- or hyposalinity; 10^5 to 10^6 years (3, 10, 42)] resulted in the regional extinction of intolerant, stenohaline species, as evidenced by the very high dissimilarity (72.8%) of the gastropod faunas (34). Halophilic species may have expanded during this time. Restriction of inflow and outflow of water at the gateway led to a slowdown of thermohaline circulation inside the basin (10^3 to 10^4 years), stratification of the water column (10^3 to 10^4 years), deoxygenation (10^4 years) (10, 43, 44), and a drop in species richness of phytoplankton (calcareous nannoplankton by 11.6% and dinocysts by 5.3%), zooplankton (planktic foraminifera by 23.4%), and nekton (bony fishes by 21.8%) (34). The time lags cannot be constrained (45) between the environmental changes and the biotic responses with a finer time resolution than the span of the pre-evaporitic Messinian or the Zanclean. Evaporation resulted in the loss of

demersal habitats, and the associated communities died out (10^3 to 10^4 years), as evidenced by the extirpation of demersal fish species (46), the drop in richness of bivalves (35.3%) (34), and the disappearance of shallow-water tropical coral reefs (16).

Gateway closure or maximum restriction

Salt precipitation started in the form of gypsum during the first stage of the MSC and became a massive accumulation of halite mainly upon the full closure or at least peak restriction of the last remaining gateway connecting the Mediterranean Sea to the world ocean (11). During the maximum restriction (or closure) stage (Fig. 3), the hydrological deficit (evaporation higher than precipitation plus riverine influx) led to base-level drawdown (at timescales of 10^3 years) (13, 47) and to the disconnection of sub-basins as a result of exposure of sills or thresholds. These events resulted in the loss of coastal habitats, which prevented population connectivity and the dispersal of larvae and plankton between coastal areas, as evidenced by the drop in species richness of ostracods (45.9%) from the Messinian to the Pliocene (34). As evaporites precipitated, the substrate became inhospitable for demersal organisms. At the final MSC stage (Lago Mare), fresh- and brackish-water influx resulted in the immigration and diversification of brackish species (1 to 10^2 years) (24).

Gateway opening

Reconnection to the global ocean allowed for the influx of larvae and individuals of previously indigenous and nonindigenous species into the Mediterranean basin, possibly in a timespan as short as months to years (48). However, this influx alone could not lead to the (re)establishment of species' populations in the Mediterranean; favorable conditions are required as well. Nutrients may have become available at surface waters much later (10^4 years), as suggested by the base-Pliocene dinocysts, which became more abundant and diversified as late as 5.08 Ma (49). A possible explanation for this is that the flood eroded and mobilized salt deposits and this led to stratification of the Mediterranean water column, thus delaying the establishment of phytoplankton populations (50). The timescale of the return to normal marine conditions after sea-level rise, as estimated from open ocean salinities (Fig. 2) (51), was even longer (10^5 years) (49, 50, 52), resulting in further delay in the establishment of foraminifera species (11). Restoration of marine conditions contributed to the formation of pelagic and demersal habitats, which allowed the establishment of connected populations of coastal species (1 to 10^2 years) and seasonal migrations. Although reestablishment of species that were present before the MSC in the Mediterranean (86 species) or the Atlantic

(832 species) was important, a large proportion of the species were new to the basin, including plankton (e.g., 40.7% of planktic foraminifera species and 45.5% of dinocysts), benthos (e.g., 61.6% of benthic foraminifera, 68.7% of ostracods, and 100% of corals), and nekton (e.g., 83.7% of bony fishes) (34). Iconic species such as the great white shark and dolphins first appeared in the Mediterranean after the MSC (53).

Discussion

Even though they are regional phenomena, salt giants are associated with major global biotic events. When a salinity crisis occurs and a salt giant is formed, the physical properties of the basin and its water column change drastically and rapidly at timescales of hundreds to thousands of years (basin restriction) to thousands of years (evaporative level drawdown), ultimately outpacing the capacity of the marine biota to adapt and perturbing ecosystems in predictable ways. Because speciation requires isolation, marginal marine basins such as the Mediterranean can become biodiversity hotspots (17), although their restriction risks conversion to evaporitic basins and leads to greater extinction than origination rates, thereby reducing species richness within the region (Fig. 2). Therefore, in addition to extinction of regionally endemic species, salt giant formation would hinder origination of new species within the basin that might compensate for increased extinction rates at global scale from independent causes (54). In the case of the MSC, for example, this has resulted in global declines in the species richness of mollusks (55) and marine mammals (56) caused by the Late Miocene cooling. Similarly, the extensive, cratonic evaporite deposition that occurred during the Permian may have enhanced the impact of the Mid-Capitanian extinction (262 to 259 Ma) in marginal settings (57).

The extraction of salt from the global ocean during the formation of salt giants may have affected the evolution of marine life through the effects of global ocean salinity on climate, ocean pH, and oxygenation (58–60). Hay *et al.* (61) postulated a correlation between the formation of the Mesozoic salt giants and the expansion of planktic foraminifera and calcareous nannoplankton into the open ocean, as well as a link between the Permian extraction of salt from the oceans and the end-Permian mass extinction (251.9 Ma). Although the evolution of planktic foraminifera lineages has been broadly associated with salinity reduction in the global ocean in the Late Miocene–Early Pliocene (62), this conclusion is contested because diversification can also be attributed to cooling climate (63). By contrast, there is a clear link between salt giant formation and the end-Triassic mass extinction (201.4 Ma): Evaporite deposition removed sulfate from the

ocean just before periods of increased volcanic activity, which facilitated large-scale oceanic anoxic events during hyperthermal events that led to the mass extinction (59).

Salinity crises have occurred repeatedly throughout geologic history in restricted evaporitic basins controlled by dynamic marine gateways that result from the formation and demise of oceans by tectonic motions and sea-level changes (64, 65). Globally, at least 138 evaporitic basins have occurred from the Proterozoic until the Miocene (66). The Mediterranean salt giant is one of the most recent among the salt giants of the Neoproterozoic (Australia), Paleozoic (Siberia, United States, and northwestern Europe), Mesozoic (the Gulf of Mexico and the South Atlantic off of Brazil, Angola, and Gabon), and the Early (Iran), Middle (Red Sea), and Late Miocene (eastern Europe) (64). In terms of size, the amount of salt (halite) deposited in the Mediterranean during the MSC was smaller than those salt giants reported from the Early Cretaceous and the Middle to Late Jurassic (61). However, the way in which the MSC reshaped Mediterranean ecosystems provides a precise quantification of biotic recovery from ecological crises. Transferring our model (Fig. 3) to other salt giants will lead to adjustments in regional geographic, geologic, oceanographic, and climatic frameworks.

REFERENCES AND NOTES

1. K. J. Hsü, W. B. F. Ryan, M. B. Cita, *Nature* **242**, 240–244 (1973).
2. W. Krijgsman, F. J. Hilgen, I. Raffi, F. J. Sierro, D. S. Wilson, *Nature* **400**, 652–655 (1999).
3. G. Aloisi *et al.*, *Geochim. Cosmochim. Acta* **327**, 247–275 (2022).
4. O. M. Bialik, M. Frank, C. Betzler, R. Zammit, N. D. Waldmann, *Sci. Rep.* **9**, 8842 (2019).
5. F. Bullian, F. J. Sierro, S. Ledesma, F. J. Jiménez-Espejo, M.-A. Bassetti, *Mar. Geol.* **434**, 106430 (2021).
6. R. Flecker *et al.*, *Earth Sci. Rev.* **150**, 365–392 (2015).
7. W. Capella *et al.*, *Earth Sci. Rev.* **180**, 37–59 (2018).
8. R. M. Ebner, F. Bullian, F. J. Sierro, T. J. Kouwenhoven, P. Th. Meijer, *Mar. Geol.* **470**, 107270 (2024).
9. F. Bullian, F. J. Jiménez-Espejo, N. Andersen, J. C. Larrasoana, F. J. Sierro, *Global Planet. Change* **231**, 104297 (2023).
10. G. Kontakiotis *et al.*, *Palaeogeogr. Palaeoclimatol. Palaeoecol.* **592**, 110903 (2022).
11. M. Roveri *et al.*, *Mar. Geol.* **352**, 25–58 (2014).
12. D. Garcia-Castellanos *et al.*, *Nature* **462**, 778–781 (2009).
13. H. Heida *et al.*, *Basin Res.* **34**, 50–80 (2022).
14. B. Haq, C. Gorini, J. Baur, J. Moneron, J.-L. Rubino, *Global Planet. Change* **184**, 103052 (2020).
15. C. N. Bianchi *et al.*, in *Life in the Mediterranean Sea: A Look at Habitat Changes*, N. Stambler, Ed. (Nova Science, 2012); pp. 1–56.
16. C. Perrin, F. R. Bosellini, *C. R. Palevol* **12**, 245–255 (2013).
17. M. Coll *et al.*, *PLOS ONE* **5**, e11842 (2010).
18. P. Koleff, K. J. Gaston, J. J. Lennon, *J. Anim. Ecol.* **72**, 367–382 (2003).
19. W. Ulrich, M. Almeida-Neto, *Ecography* **35**, 865–871 (2012).
20. K. Agiadi *et al.*, Revised marine fossil record of the Mediterranean before and after the Messinian Salinity Crisis, Zenodo (2024); <https://doi.org/10.5281/zenodo.12698765>.
21. K. Agiadi *et al.*, A revised marine fossil record of the Mediterranean before and after the Messinian Salinity Crisis, Earth System Science Data (2024); <https://doi.org/10.5194/essd-2024-75>.
22. A. S. Madof, C. Bertoni, J. Lofi, *Geology* **47**, 171–174 (2019).

23. Z. Gvirtzman *et al.*, *Geology* **45**, 915–918 (2017).
24. F. Andreotto *et al.*, *Earth Sci. Rev.* **216**, 103577 (2021).
25. A. S. Madof *et al.*, *Terra Nova* **34**, 395–406 (2022).
26. G. Carnevale, W. Schwarzhans, *Riv. Ital. Paleontol. Stratigr.* **128**, 283–324 (2022).
27. K. Mužek *et al.*, *Palaeogeogr. Palaeoclimatol. Palaeoecol.* **632**, 111847 (2023).
28. A. Grothe, F. Sangiorgi, H. Brinkhuis, M. Stoica, W. Krijgsman, *Newsl. Stratigr.* **51**, 73–91 (2018).
29. K. Agiadi *et al.*, Biogeographic data for “The marine biodiversity impact of the Late Miocene Mediterranean salinity crisis,” Zenodo (2024); <https://doi.org/10.5281/zenodo.12796724>.
30. G. Aiello, R. Parisi, R. Barbieri, D. Barra, *Palaeogeogr. Palaeoclimatol. Palaeoecol.* **643**, 112155 (2024).
31. W. Schwarzhans, *Swiss J. Paleontol.* **142**, 4–85 (2023).
32. G. Carnevale *et al.*, *Boll. Soc. Paleontol. Ital.* **58**, 109–140 (2019).
33. D. V. Palcu, L. A. Golovina, Y. V. VERNYHOROVA, S. V. Popov, W. Krijgsman, *Global Planet. Change* **158**, 57–71 (2017).
34. K. Agiadi *et al.*, Late Miocene transformation of Mediterranean Sea biodiversity. bioRxiv 585031 [Preprint] (2024); <https://doi.org/10.1101/2024.03.14.585031>.
35. M. Harzhauser, A. Guzhov, B. M. Landau, A. K. Kern, T. A. Neubauer, *Palaeogeogr. Palaeoclimatol. Palaeoecol.* **630**, 111811 (2023).
36. I. Cornacchia, M. Brandano, S. Agostini, *Earth Sci. Rev.* **221**, 103785 (2021).
37. F. F. Steininger, F. Rögl, *Spec. Publ. Geol. Soc. Lond.* **17**, 659–668 (1984).
38. S. V. Popov *et al.*, *Cour. Forsch. Inst. Senckenberg* **250**, 1–46 (2004).
39. W. Schwarzhans, K. Agiadi, G. Carnevale, *Riv. Ital. Paleontol. Stratigr.* **126**, 657–724 (2020).
40. A. Mondanaro, S. Dominici, S. Danise, *Palaeontology* **67**, e12696 (2024).
41. A. Darnaude *et al.*, *Res. Ideas Outcomes* **8**, e80223 (2022).
42. I. Vasiliev *et al.*, *Paleoceanogr. Paleoclimatol.* **34**, 182–202 (2019).
43. A. M. Mancini *et al.*, *Deep Sea Res. Part I Oceanogr. Res. Pap.* **203**, 104217 (2024).
44. B. Alhammoud, P. T. Meijer, H. A. Dijkstra, *Paleoceanography* **25**, PA2220 (2010).
45. J. B. C. Jackson, A. O’Dea, *Proc. Natl. Acad. Sci. U.S.A.* **120**, e2307520120 (2023).
46. K. Agiadi *et al.*, *Biogeosciences* **2024**, (2024).
47. P. Th. Meijer, W. Krijgsman, *Earth Planet. Sci. Lett.* **240**, 510–520 (2005).
48. D. Garcia-Castellanos *et al.*, *Earth Sci. Rev.* **201**, 103061 (2020).
49. L. Londeix, M. Benzakour, J.-P. Suc, J.-L. Turon, *Geobios* **40**, 233–250 (2007).
50. U. Amarathunga *et al.*, *Nat. Geosci.* **15**, 720–725 (2022).
51. F. Filade *et al.*, *Palaeogeogr. Palaeoclimatol. Palaeoecol.* **631**, 111831 (2023).
52. G. Kontakiotis *et al.*, *Palaeogeogr. Palaeoclimatol. Palaeoecol.* **459**, 348–364 (2016).
53. G. Bianucci *et al.*, *Geobios* **44**, 549–585 (2011).
54. A. L. Stigall, J. E. Bauer, A. R. Lam, D. F. Wright, *Global Planet. Change* **148**, 242–257 (2017).
55. P. Monegatti, S. Raffi, *Palaeogeogr. Palaeoclimatol. Palaeoecol.* **297**, 1–11 (2010).
56. C. M. Peredo, M. D. Uhen, *Palaeogeogr. Palaeoclimatol. Palaeoecol.* **449**, 227–235 (2016).
57. B. P. Smith, T. Larson, R. C. Martindale, C. Kerans, *Earth Planet. Sci. Lett.* **530**, 115876 (2020).
58. I. Halevy, A. Bachan, *Science* **355**, 1069–1071 (2017).
59. T. He *et al.*, *Sci. Adv.* **6**, eabb6704 (2020).
60. S. Olson, M. F. Jansen, D. S. Abbot, I. Halevy, C. Goldblatt, *Geophys. Res. Lett.* **49**, e2021GL095748 (2022).
61. W. W. Hay *et al.*, *Palaeogeogr. Palaeoclimatol. Palaeoecol.* **240**, 3–46 (2006).
62. B. A. Malmgren, W. A. Berggren, *Paleoceanography* **2**, 445–456 (1987).
63. K.-Y. Wei, J. P. Kennett, *Paleoceanography* **1**, 67–84 (1986).
64. J. K. Warren, *Earth Sci. Rev.* **98**, 217–268 (2010).
65. D. Garcia-Castellanos, A. Villaseñor, *Nature* **480**, 359–363 (2011).
66. Z. J. Qin *et al.*, Large Evaporite Provinces: Geothermal rather than solar origin? Research Square [Preprint] (2020); <https://doi.org/10.21203/rs.3.rs-80284/v1>.
67. N. Hohmann, K. Agiadi, Code for: The marine biodiversity impact of the Late Miocene Mediterranean salinity crisis, Zenodo (2024); <https://doi.org/10.5281/zenodo.12678336>.
68. N. Hohmann, K. Agiadi, Code for: A revised marine fossil record of the Mediterranean before and after the Messinian Salinity Crisis, Zenodo (2024); <https://doi.org/10.5281/zenodo.10782803>.
69. J. Lofi, Atlas Contributors Team, Seismic atlas of the “Messinian Salinity Crisis” markers in the Mediterranean Sea (Commission for the Geological Map of the World/Mémoires de la Société Géologique de France, 2014).
70. A. Tzanova, T. D. Herbert, L. Peterson, *Earth Planet. Sci. Lett.* **419**, 71–80 (2015).
71. T. D. Herbert *et al.*, *Nat. Geosci.* **9**, 843–847 (2016).

ACKNOWLEDGMENTS

The authors wish to dedicate this study to the memory of Prof. Maria Bianca Cita Sironi. We thank A. Fuster for her helpful comments on the methods. This is Ismar-CNR, Bologna, scientific

contribution number 2092. Views and opinions expressed are exclusively those of the author(s) and do not necessarily reflect those of the European Union or the European Research Council. Neither the European Union nor the granting authority can be held responsible for them. **Funding:** This was supported by the Austrian Science Fund (FWF grant V986-N to K.A.); the European Union (ERC, MindTheGap, StG project 101041077 to N.H.); COST (action CA15103 to K.A., D.T., F.R.B., F.L., A.M.M., G.K., E.B., S.D.Z., M.H., F.J.S., I.V., A.C., and D.G.-C.); Severo Ochoa Centre of Excellence (accreditation CEX2019-00928-S to M.C.); and the European Commission (ITN SaltGiant Horizon 2020-765256 to F.B., F.J.S., A.C., and D.G.-C.). **Author contributions:** Conceptualization: K.A., D.G.-C.; Data curation: K.A., N.H.; Formal analysis: N.H.; Funding acquisition: K.A., M.C., A.Ca., D.G.-C.; Investigation: K.A., N.H., E.G., D.T., F.R.B., M.T., G.B., A.Co., L.L., C.F., F.B., E.K., F.L., A.M.M., S.D., P.M., I.B.C., E.B., G.I., A.A., G.K., E.B., S.D.Z., M.H., F.J.S.; Methodology: K.A., N.H.; Project administration: K.A.; Visualization: K.A., N.H., I.V., D.G.-C.; Writing – original draft: K.A., D.G.-C.; Writing – review & editing: N.H., E.G., D.T., F.R.B., M.T., G.B., A.Co., L.L., C.F., F.B., E.K., F.L., A.M.M., A.A., G.K., E.B., S.D.Z., M.H., F.J.S., M.C., I.V., A.Ca. **Competing interests:** The authors declare no competing interests. **Data and materials availability:** All data are available in the main text or the supplementary materials. The dataset used for the present analysis is publicly available under a CC BY license in (20), and details on how the dataset was compiled can be found in (21). The paleobiogeographic data used to infer the possible endemic species are available in (29). All code used in the analysis is available in (67). The code to map the localities that was used to produce Fig. 1 is available in (68). **License information:** Copyright © 2024 the authors, some rights reserved; exclusive licensee American Association for the Advancement of Science. No claim to original US government works. <https://www.science.org/about/science-licenses-journal-article-reuse>. This research was funded in whole or in part by the Austrian Science Fund (FWF) Grant DOI 10.55776/V986, a coAllition S organization. The author will make the Author Accepted Manuscript (AAM) version available under a CC BY public copyright license.

SUPPLEMENTARY MATERIALS

science.org/doi/10.1126/science.adp3703
Materials and Methods
Supplementary Text
Fig. S1
Table S1
References (72–150)
MDAR Reproducibility Checklist

Submitted 21 March 2024; accepted 31 July 2024
10.1126/science.adp3703